Link between Organ-specific Antigen Processing by 20S Proteasomes and CD8$^+$ T Cell–mediated Autoimmunity

Ulrike Kuckelkorn,[1] Thomas Ruppert,[1] Britta Strehl,[1] Peter R. Jungblut,[2] Ursula Zimny-Arndt,[2] Stephanie Lamer,[2] Immo Prinz,[2] Ilse Drung,[1] Peter-M. Kloetzel,[1] Stefan H.E. Kaufmann,[2] and Ulrich Steinhoff[2]

[1]*Institute of Biochemistry, Charite, Humboldt University, and* [2]*Max-Planck Institute for Infection Biology, D-10117 Berlin, Germany*

Abstract

Adoptive transfer of cross-reactive HSP60-specific CD8$^+$ T cells into immunodeficient mice causes autoimmune intestinal pathology restricted to the small intestine. We wondered whether local immunopathology induced by CD8$^+$ T cells can be explained by tissue-specific differences in proteasome-mediated processing of major histocompatibility complex class I T cell epitopes. Our experiments demonstrate that 20S proteasomes of different organs display a characteristic composition of α and β chain subunits and produce distinct peptide fragments with respect to both quality and quantity. Digests of HSP60 polypeptides by 20S proteasomes show most efficient generation of the pathology related CD8$^+$ T cell epitope in the small intestine. Further, we demonstrate that the organ-specific potential to produce defined T cell epitopes reflects quantities that are relevant for cytotoxic T lymphocyte recognition. We propose tissue-specific antigen processing by 20S proteasomes as a potential mechanism to control organ-specific immune responses.

Key words: antigen processing • proteasomes • intestinal mucosa • T cell epitopes • autoimmunity

Introduction

Understanding of organ-specific autoimmune diseases is hampered by a dilemma: although some autoantigens are ubiquitously expressed, they provoke local pathogenic immune responses (1, 2). A healthy organism presents autologous peptides which are normally tolerated or ignored by peripheral T lymphocytes. Microbial infections, mutations of cellular proteins or failure in immunoregulation can activate CD8$^+$ T cells causing organ-specific autoimmune pathology. We have established mycobacterial HSP60-specific CD8$^+$ T cells that cross react with the murine homologue. HSP60 peptides of either mycobacterial ($AA_{499–508}$: SALQNAASIA) or murine origin ($AA_{162–171}$: KDIGNIISDA) are recognized in a H-2D^b–restricted fashion (3). While these cross-reactive T cells did not cause pathology in immunocompetent mice, adoptive transfer into immunodeficient mice resulted in organ-specific inflammation of the small intestine but not the colon, despite comparable migration in both tissues, and elevated expression of murine heat shock protein 60 (mu HSP60)* in the colon (2). We therefore wondered whether different tissues exhibit differences in their capacity to process MHC class I antigens.

MHC class I molecules are ubiquitously expressed surface molecules which bind peptides of 8–10 amino acids for display to the T cell system. These peptides are antigenic side products in the continual turnover of intracellular proteins, mostly originating from ubiquitin-tagged proteins (4). Most of these peptides are generated by 26S proteasomes, the major proteolytic enzyme machinery of a cell (5, 6). Although other proteases with selective cleavage specificity might also contribute to the MHC class I peptide pool, this seems to apply only for a limited subset of peptides and cannot substitute for proteasome function (7).

The proteolytic active sites of the 26S proteasomes are housed within the 20S core complex that is composed of four stacked rings with seven subunits each. The outer rings contain the α-subunits (α1–α7) which shape the gates of substrate entry and product release. The two inner rings harbor the β subunits (β1–β7) of which three β-subunits, β1, β5, and β2 are catalytically active (8). Stimulation with

Address correspondence to U. Steinhoff, Max-Planck Institute for Infection Biology, Schumannstr. 21/22, D-10117 Berlin, Germany. Phone: 49-30-28460-525; Fax: 49-30-28460-503; E-mail: steinhoff@mpiib-berlin.mpg.de

*Abbreviations used in this paper: 2-DE, two-dimensional gelelectrophoresis; MALDI-MS, matrix-assisted laser desorption-ionization mass spectrometry; mu HSP60, murine heat shock protein 60; pI, isoelectric point.

IFN-γ results in an exchange of these constitutive β subunits with the inducible iβ1 (LMP2), iβ5 (LMP7), and iβ2 (MECL-1) subunits leading to the formation of immunoproteasomes (9–11). Cytokine-induced subunit exchange occurs during proteasome assembly and profoundly alters the cleavage specificity of 20S proteasomes (12, 13).

To investigate whether tissue-restricted pathology is influenced by organ-specific processing of MHC class I ligands, we analyzed the subunit composition of 20S proteasomes from various organs and compared their ability to generate peptides and T cell epitopes which are involved in the induction of organ-specific pathology of the small intestine.

Materials and Methods

Mice. Mice were bred in the animal facilities of the Max-Planck Institute at the Bundesamt für gesundheitlichen Verbraucherschutz und Veterinärmedizin (BgVV) under specific pathogen-free conditions.

Proteasome Purification. 20S proteasomes were isolated from the liver, small intestine, colon, spleen, and thymus of normal C57BL/6 mice. These mice were chosen because 20S proteasomes subunit composition did not differ from α/β T cell–deficient (β $TCR^{-/-}$) mice, which develop pathology (2). Organs were carefully rinsed and frozen in liquid nitrogen. The tissues were homogenized in 5 to 10 volumes of lysis buffer containing 20 mM Tris, pH 7.2, 1 mM EDTA, 1 mM NaN_3, 1 mM DTT, 50 mM NaCl, 0.1% NP-40 supplemented with 4 mM PMSF, 2 μM Pepstatin, 2 μM Leupeptin, 0.6 μM Aprotinin, 13 μM Bestatin, 10 and 100 μg/ml trypsin inhibitor (fourfold higher concentrations of PMSF and trypsin inhibitor were used for lysis of small intestines). Filtered lysates were applied onto DEAE Sephacel (Amersham Pharmacia Biotech) and carefully washed with 50 and 150 mM NaCl until no protein was detected by UV absorption (280 nm). Proteasomes were eluted with 350 mM NaCl in TEAD (20 mM Tris, pH 7.2, 1 mM DTT) buffer and concentrated by ammonium sulfate precipitation between 40 to 70% saturation. Protein fractions were separated by ultra centrifugation on sucrose gradients (10 to 40%) and ultracentrifuged at 40,000 rpm for 16 h in a Beckman Coulter SW40 rotor. Fractions containing proteasomes were pooled and applied to a MonoQ® column (FPLC Pharmacia) and eluted with a linear gradient of 100 to 500 mM NaCl in TEAD. The reproducibility of the 20S proteasome purification and the 2D-gel protein pattern was confirmed by four independent experiments.

Protease Assay. The proteolytic activity of the proteasomes was tested with the synthetic peptide substrate Suc-LLVY-MCA. The assay was performed in a 100 μl reaction volume containing 100 ng proteasome, 50 mM Tris/Cl, pH 7.5, 10 mM NaCl, 30 mM KCl, 0.1 mM EDTA, and 20 μM substrate. Fluorescence was detected by fluorescence microtiter reader Fluostar (TECAN®) at 390 nm excitation/460 nm emission for MCA.

Peptide Digest. To determine 20S proteasome mediated cleavage of synthetic peptides, 20 μg of a 30 mer peptide derived from the mu HSP60 (VATISANGDKDIGNIISDAMKKVGRKGVIT) were incubated at 37°C for 1 to 20 h with 2 μg of the purified 20S proteasomes in buffer containing 20 mM Hepes/KOH, pH 7.8; 2 mM Mg-acetate; 2 mM DTT in a total volume of 300 μl. Reactions were stopped by adding TFA to a final concentration of 0.1% or by freezing at −70°C.

Peptide Analysis and Quantification. Samples were analyzed by reverse phase HPLC (RP-HPLC), system HP1100 (Hewlett-Packard) equipped with a RPC C2/C18 SC 2.1/10 column (Amersham Pharmacia Biotech). A gradient of eluent A (0.05% TFA) and eluent B (80% acetonitrile, 0.05% TFA) between 5–63% B was run in 30 min, followed by 63–95% B in 4 min; with a flow rate of 50 μl/min. Analysis was performed on-line with a LCQ ion trap MS (ThermoQuest) equipped with an electrospray ion source. Each scan was acquired over the range m/z 300–1300 in 3 s. Peptides were identified by their molecular masses calculated from the m/z peaks of the single or multiple charged ions and were confirmed by tandem mass spectrometry (MS) sequencing analyses. The strongest electric signal induced by an individual peptide generated by organ derived 20S proteasomes was defined as 1.

Two-Dimensional Gelelectrophoresis and Spot Identification by MS. For resolution of 20S proteasomal proteins, we combined isoelectric focusing by carrier ampholytes with SDS-PAGE (14). We applied 60 μg of protein to the anodic side of a carrier ampholyte IEF gel. In the second dimension, proteins were separated in 1.5 mm thick SDS-PAGE gels (23 cm × 30 cm) and stained by Coomassie Brilliant Blue G250. For identification, individual spots were cut out, digested by trypsin, desalted and concentrated by ZIPTIP, and analyzed by matrix-assisted laser desorption-ionization mass spectrometry (MALDI-MS) as recently described (15).

^{51}Cr-release Assay. CTL activities of HSP60-specific T cells were measured in a ^{51}Cr release assay using EL4 cells as targets as described previously (3). Cloned T cells were incubated with 2×10^3 ^{51}Cr-labeled EL4 cells in the presence of 20 μl HSP60 substrate digests by 20S proteasomes from various organs for 4 h at 37°C in 7% CO_2 at various effector/target ratios. After 4 h, 100 μl of the supernatant was removed and measured in a gamma counter. Percent specific lysis was calculated as follows: (experimental ^{51}Cr-release − spontaneous ^{51}Cr-release) × 100/(maximum ^{51}Cr-release − spontaneous ^{51}Cr-release).

Histology. Examination of histopathology was performed with tissues from naive and T cell reconstituted mice. Tissues were fixed in 4% PFA, dehydrated in cold acetone, and embedded into Kulzer Technovit 8100 (Haereus Kulzer) following the manufacturer's instructions. After polymerization, sections were cut at 3 μm on a rotation microtome (Leica) and stained with hematoxylin and eosin. Tissues were graded in a blinded fashion from a pathologist according to signs of T cell infiltrations, mucosa thickening, hemorrhage, and epithelial cell integrity. Immunohistochemistry was performed on cryostat sections that have been blocked with PBS containing 5% mouse serum and then incubated with the primary antibody (anti-Vβ8.1, 8.2-FITC) for 60 min. Secondary Ab incubation was performed with rat anti-FITC peroxidase-conjugated mAb (Boehringer). Endogenous peroxidase was blocked with 3% H_20_2 for 2 min, and staining was visualized by addition of 3-amino-9-ethylcarbazole (Dakopatts) as substrate. Phosphate-buffered saline was used for washing steps between the antibody incubations. Specificity of staining was checked with isotype-matched control mAbs.

Results and Discussion

Subunit Composition of 20S Proteasomes from Various Tissues. To determine whether the composition of the 20S core proteasomes differs between various tissues, we isolated 20S proteasomes from liver, thymus, small intestine, and colon by two-dimensional gelelectrophoresis (2-DE) and identified proteins by MALDI-MS. Marked differences

between individual organs were observed including both β-subunits as well as α-subunits of the 20S proteasome (Fig.1, A–D). Focusing specifically on the model of the intestinal autoimmune pathology, a detailed MALDI-MS analysis of the 20S proteasome subunits from the small intestine and the colon were performed. The results of this analysis are listed in Table I. In the small intestine, the α4 subunit was identified in three spots (α4.1–α4.3) showing similar molecular mass (Mr) but different isoelectric points (pI), suggesting posttranslational modifications as a cause for this polymorphism. While these variant forms were present with similar intensities in the colon, the α4.2 and α4.3 were markedly reduced in the small intestine. The α6 subunit was detected in three spots which differed not only in the pI but also in their relative Mr. In the small intestine, the α6 variants were present in equimolar ratios, whereas in the colon the α6.1 dominated over the α6.2 and α6.3 variants which were only marginally present, comparable to the liver (Fig. 1, A–D). These polymorphisms in the subunit composition of 20S proteasomes may be due to tissue specific functional modifications, including differential transcription and posttranslational modification as has been discussed previously (16–18).

Notably, the α4 and α6 subunits are known to interact with the proteasomal regulatory complexes PA700 and PA28 and additional proteins of cellular and viral origin (19, 20). It is therefore assumed that protein interactions with the α4 and α6 subunits may modulate the activity of the 20S proteasome by controlling substrate entry into the catalytic cavity (21).

The proteasomes of different tissues also revealed a characteristic composition of β-subunits. The immunoproteasome subunits iβ1, iβ2, and iβ5 were predominantly found in the small intestine and the thymus, whereas high amounts of the constitutive proteasome subunits β1, β2, and β5 were detected in proteasomes of the colon and the liver. However, most prominent differences were observed for the β2 subunit which varied with respect to the pI and size between the organs analyzed. While the ratio of β2 and iβ2 expression was similar in the colon and in the liver, increased amounts of the iβ2 subunit and lowered level of β2 was observed in the thymus and the small intestine. Interestingly, the subunits of the latter organs focused at a more basic pI (Fig. 1, A–D, right panel). The molecular basis of this shift is not yet clear.

Generation of HSP60 Cleavage Fragments and T Cell Epitopes. To examine the potential consequences of organ-specific proteasome subunit composition, we first compared the generation of distinct cleavage fragments of the mu HSP60 substrate by organ-derived 20S protea-

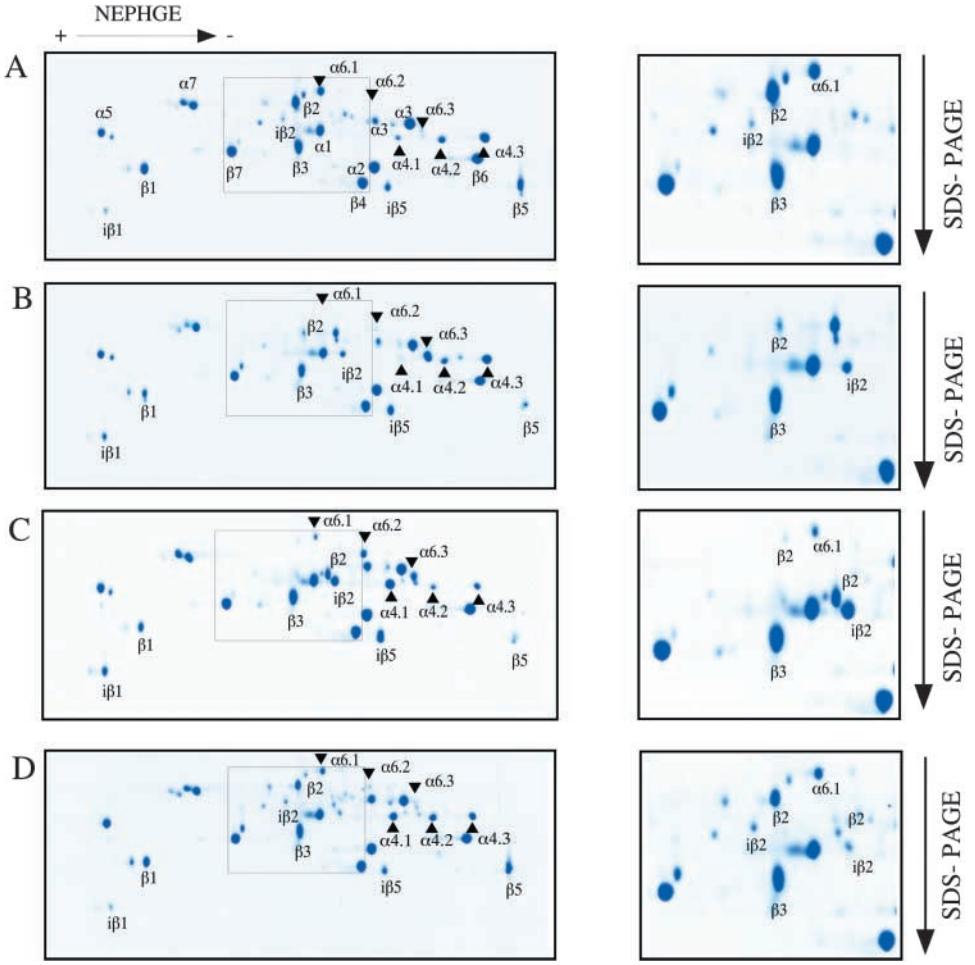

Figure 1. The subunit composition of 20S proteasomes varies between different organs. Purified 20S proteasomes were analyzed by 2-DE and MS identified spots of the thymus, small intestine, and colon were compared with proteasomes subunits of the liver. Identification of the main subunits in the liver (A). Differences in α subunits of thymus (B), small intestine (C), and colon (D) were marked by black triangles. The β immunosubunits (iβ) and the corresponding constitutive subunits (β) are indicated. The right panel depicts an enlarged view of the indicated area in the 2-DE. Note that β2 and iβ2 subunits differ in their relative M_r and pI. To ensure reproducibility, four individual preparations of 20S proteasomes were performed for each organ.

Table I. *Subunit Differences of 20S Proteasomes from the Small Intestine and Colon*

α-Subunits	Gene	Spot	Small intestine	Colon
α1 (Jota)	PSMA 6	α1	+	+
α2 (C3)	PSMA 2	α2	+	+
α3 (C9)	PSMA 4	α3.1/α3/2	+	+
α4 (C6)	PSMA 7	α4.1		
		α4.2		
		α4.3	α4.1 > α4.2 > α4.3	α4.1 = α4.2 = α4.3
α5 (Zeta)	PSMA 5	α5	+	+
α6 (C2)	PSMA 1	α6.1		
		α6.2		
		α6.3	α6.3 > α6.2 > α6.1	α6.1 > α6.2 > α6.3
α7 (C8)	PSMA 3	α7	+	+
β-Subunits				
β1 (delta)	PSMB 6	β1	+	++
iβ1 (LMP2)	PSMB 9	iβ1	++	(+)
β2 (Z)	PSMB 7	β2 (anodic)	−	++
		β2 (cathodic)	++	(+)
iβ2 (MECL1)	PSMB 10	iβ2 (anodic)	−	+
		iβ2 (cathodic)	++	(+)
β3 (C10)	PSMB 3	β3	+	+
β4 (C7)	PSMB 2	β4	+	+
β5 (MB1)	PSMB 5	β5	(+)	++
iβ5 (LMP7)	PSMB 8	iβ5	++	(+)
β6 (C5)	PSMB 1	β6	+	+
β7 (N3)	PSMB 4	β7	+	+

α- and β-subunits of 20S proteasomes isolated from small intestines and colons were compared and evaluated: = comparable amounts; (+) traces; − not detectable; + normal intensity; ++ increased intensity. β2 and iβ2 were detected in two isoforms differing in their IP (anionic and cathodic, respectively). The basic isoforms of β2 and iβ2 were strongly expressed in the small intestine and only marginally in the colon and thymus.

somes. Therefore, 20S proteasomes isolated from various tissues were normalized according to their protein amount since the adjustment of tissue derived 20S proteasomes based on their hydrolytic activity against short fluorogenic peptide substrates strongly depends on the content of immunosubunits (22). The purity of 20S proteasomes was assessed by native PAGE followed by fluorogenic substrates overlay, which excludes the copurification of contaminating proteases. Sequence information of cleavage products was obtained by tandem MS. The main cleavage products of the mu HSP60 from tissue derived proteasomes are summarized in Table II. Although there were few qualitative

Table II. *Proteasomal Cleavage Products (Differ between Organs)*

Cleavage products											
1	5	10	15	20	25	30	Organs				
VATISANGDKDIGNIISDAMKKVGRKGVIT							SI	C	L	SP	T
VATIS							0.7	0.2	0.5	0.5	**1.0**
VATISA							**1.0**	0.3	**1.0**	0.5	**0.9**
VATISANGD							**0.8**	0.2	0.5	0.6	1.0
	SANGDKDIGNIISD						**1.0**	0.1	0.1	0.2	0.5
		NGDKDIGNIISDAMKKVGRKGVIT					**1.0**	0.3	**0.8**	0.4	**0.9**
			KDIGNIISD				**1.0**	0.1	0.2	0.1	0.5
						KVGRKGVIT	0.7	0.6	0.2	**1.0**	**0.9**
						VGRKGVIT	**1.0**	**0.8**	0.1	0.1	0.1
						KGVIT	0.6	**1.0**	0.1	0.1	0.1

The mu HSP60 substrate (VATISANGDKDIGNIISDAMKKVGRKGVIT) was digested by isolated 20S proteasomes from various organs (SI, small intestine; C, colon; L, liver; SP, spleen and T, thymus). Peptide sequences were analyzed by MS, maximal signal intensities of individual peptides were arbitrarily defined as 1.0. Main cleavage products of the mu HSP60 substrate are listed and the relative amounts generated by individual organs are shown to the right.

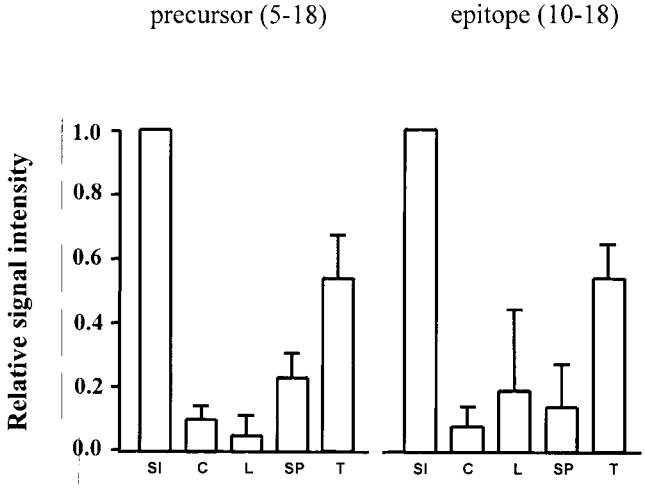

Figure 2. Generation of organ-specific peptide fragments by 20S proteasomes. The mu HSP60 substrate (VATISANGDKDIGNIISDAMKKVGRKGVIT) was digested by isolated 20S proteasomes from various organs (SI, small intestine; C, colon; L, liver; SP, spleen and T, thymus). Peptide sequences were analyzed by MS, maximal signal intensities of individual peptides were arbitrarily defined as 1.0. Relative amounts of a potential precursor (5–18) and the T cell epitope (10–18) of the mu HSP60. Data from three experiments, means ± SD are shown.

differences in cleavage products, some tissues varied markedly in the quantity of peptides generated. The quantitative assignment of peptides to individual organs shows, that the majority of fragments were most efficiently produced by tissues expressing high levels of immunosubunits, i.e., the small intestine and thymus. However, despite the fact that the small intestine and the thymus express comparable levels of immunoproteasomes, they differed significantly in their cleavage site preferences. As proteasomes of the small intestine and the thymus differed only in their α-subunit composition as described in Table I, these data indicate that modifications in the α-subunits of 20S proteasomes may also influence their processing characteristics.

With respect to the localized inflammation mediated by HSP60-specific T cells, we next analyzed the ability of 20S proteasomes from various tissues to generate epitopes of the mu HSP60 polypeptide substrate. Although one can assume that in vivo most of the antigens are processed by the 26S proteasomes it has been demonstrated for a large number of viral and tumor antigens that in vitro processing of polypeptide substrates containing MHC class I epitopes by 20S proteasomes closely resembles the situation in living cells (for a review, see reference 23). Nevertheless, as in vitro data suggested differences in the generation of cleavage fragments between 20S and 26S proteasomes (24), we investigated whether both types of proteasomes were able to generate the mu HSP60 T cell epitope. MS analyses revealed generation of the pathology relevant epitope by the 20S as well as the 26S proteasomes supporting the relevance of the data obtained with purified 20S proteasomes (data not shown). Fig. 2 summarizes the relative abundance of T cell epitopes produced by organ derived 20S proteasomes. The mu HSP60 T cell epitope KDIGNIISD and NH_2-terminally elongated fragments which could serve as precursors were generated in a significantly more efficient way by the small intestine compared with the colon. Similar results demonstrating organ-specific preferences in cleavage site usage were also obtained with a polypeptide substrate derived from the pp89 protein of the murine cytomegalovirus (data not shown).

Recognition of In Vitro Generated Epitopes by HSP60-specific CTLs Correlates with the Intestinal Pathology of T Cell Reconstituted β $TCR^{-/-}$ Mice. To show that peptides were exclusively processed by 20S proteasomes and not by contaminating cytosolic proteases, in vitro digests of the mu HSP60 were performed in the presence of the proteasome inhibitor MG 132 or an inhibitor of the cytosolic tripeptidyl peptidases II, AAF-CMK. The HPLC-profiles reveal that peptide fragmentation of the mu HSP60 substrate was mediated by 20S proteasomes and not by contaminating proteases (Fig. 3 A).

We next investigated whether in vitro–generated epitopes were of functionally relevant amounts and quality. To this end, recognition of HSP60 digests was determined in a ^{51}Cr release assay. Studies with overlapping peptides revealed that the epitopes KDIGNIISDA and KDIGNIISD of the mu HSP60 were recognized by T cells at physiological concentrations of 10^{-10} M (3). Target cells pulsed with cleavage products derived from 20S proteasomes of the small intestine but not from other organs were lysed by HSP60-specific T cells (Fig. 3 B). Specific recognition of the mu HSP 60 T cell epitope in the small intestine but not the colon is in accordance with the pathology observed in HSP60 T cell–reconstituted β $TCR^{-/-}$ mice. Cross sections of the small intestines revealed hemorrhage and immense expansion of HSP60-specific T cells in the lamina

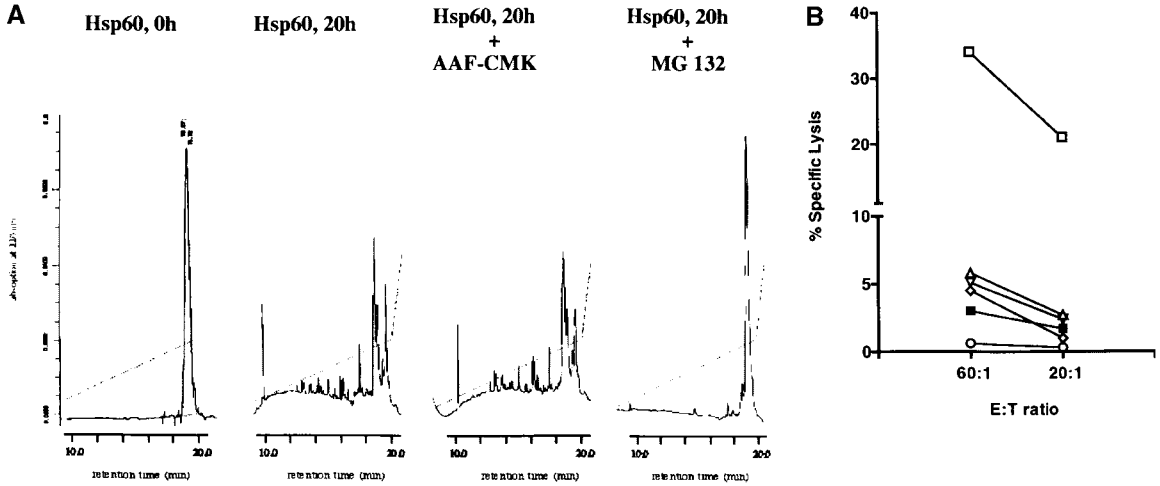

Figure 3. HSP60-specific T cells recognize peptides generated by 20S proteasomes from the small intestine. (A) HPLC profiles of a 30 mer peptide of HSP60 before digestion (HSP60, 0 h), after proteasomal digestion for 20 h (HSP60, 20h), after proteasomal digestion for 20 h in the presence of 3 μM tripeptidyl peptidase inhibitor AAF-CMK (HSP60, 20h + AAF-CMK) and the proteasomes inhibitor MG 132 (HSP60, 20h + MG 132), respectively. (B) Cytolytic activity of a cross-reactive HSP60-specific T cell clone was measured in a ^{51}Cr-release assay on EL-4 cells loaded with equal amounts of digests (20 μl) of HSP60 performed by 20S proteasomes from the small intestine (□), the liver (△), the colon (◇), the thymus (▽) or left untreated (○). EL-4 cells were loaded with digests performed by small intestinal 20S proteasomes in the presence of 3 μM proteasome inhibitor MG132 (■).

propria and epithelium leading to the destruction of the apical epithelial barrier (Fig. 4 C). In contrast, despite the fact that HSP60-specific T cells were also found in the colon, immunopathology did not develop in this tissue (Fig. 4, D–F).

Mammalian proteasomes generate with high accuracy the COOH-terminal residues of MHC class I peptides. Often, however, antigenic peptides are not generated as 8 or 10-residue products but as NH_2-terminal extended precursor peptides that require trimming by amino peptidases (25, 26). Most of these enzymes are located in the endoplasmic reticulum, but in some rare cases cytosolic trimming has also been described. In addition, there is convincing evidence that proteasomes cleave some MHC class I ligands in a definite form (27). This is in accordance with our data showing that isolated 20S proteasomes are sufficient to cleave the T cell epitope of muHSP 60 (KDIGNIISD) at both ends, although we cannot exclude that trimming of the proteasomal precursor epitope, SANGDKDIGNIISD, also leads to the maturation of the T cell epitope.

Recently, it has been shown that muscle cells contain several 20S proteasomes subtypes which exhibit different cleavage properties. Although the biological significance of this observation remains at present unclear and requires further studies, it can be concluded that the cleavage properties of cells or organs most likely reflect the sum of different subtype activities (28). Notably, tissues (thymus, small intestine) having comparable levels of immunosubunits varied considerably in their cleavage preference. This indicates that the preferred cleavage site usage of 20S proteasomes is also influenced by isoforms of α subunits present in the organ.

Although we would like to attribute the recorded functional and structural proteasome differences to individual cell types, such experiments are currently not possible due to technical limitations. Further, isolating individual cell types from their normal microenvironment does not reflect the processing and presentation pattern of cells which reside in their physiological environment. This has recently been demonstrated by differences in antigen presentation between infected splenocytes and macrophages (29).

Our data demonstrate that 20S proteasomes are sufficient to generate the $CD8^+$ T cell epitopes of the mu HSP60 and that 20S proteasomes derived from different organs produce a distinct peptide pattern due to their organ-typic subunit composition. Therefore, generation of high quantities of self-epitopes in selected tissues may correlate with organ-specific autoimmunity. Thus, we propose that in addition to peripheral immune regulatory mechanisms, organ-specific epitope generation represents an important mechanism to control the reactivity of autoreactive $CD8^+$ T cells that escape thymic deletion. In the absence of peripheral immune regulation, processing of self-epitopes in distinct tissues may result in organ-specific pathology. This raises the general concept that proteasomal antigen processing is a further step in the control of organ-specific immune responses caused by $CD8^+$ T cells ranging from pathology to protection.

We thank P. Henklein for the peptide synthesis, V. Brinkmann for the microscopy, K. Janek for supporting the MS-analysis, and P. Seiler and P. Aichele for helpful discussions and critically reading the manuscript.

This work was in part supported by the Sonderforschungsbereich 421.

Submitted: 9 July 2001
Revised: 29 January 2002
Accepted: 12 February 2002

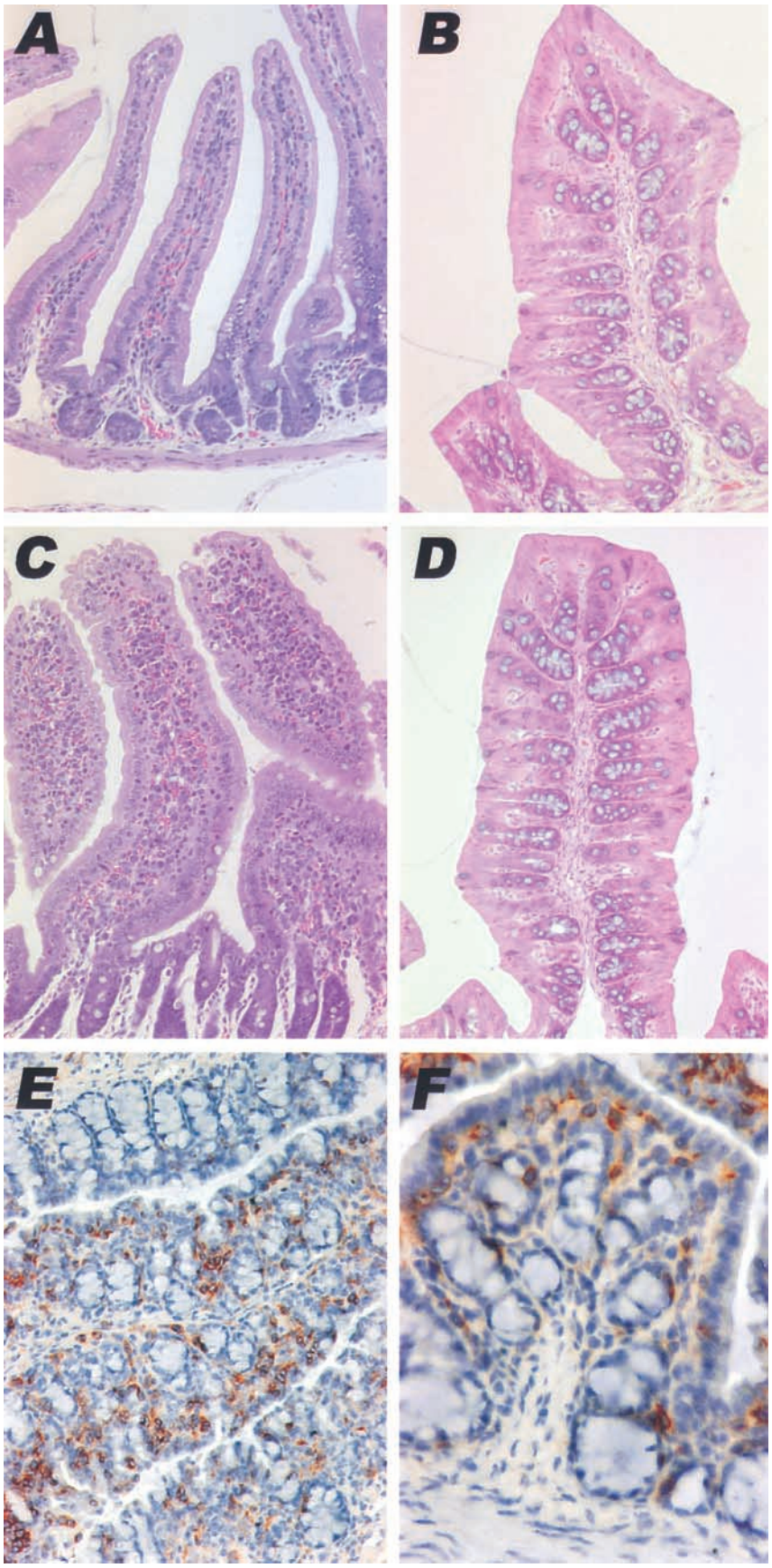

Figure 4. Transfer of HSP60-specific T cells into β $TCR^{-/-}$ mice leads to inflammation of the small intestine but not the colon. Hematoxylin and eosin stained cross sections of the naive small intestine (A) and the colon (B) and 16 d after reconstitution with HSP60-specific T cells, small intestine (C), colon (D). Cross sections of the small intestine (C) but not the colon (D) show massive expansion of HSP60-specific T cells in the lamina propria and epithelium with degenerative processes at the apical end of the villi. HSP60-specific T cells were detected 16 d after adoptive transfers in the colon by staining for Vβ8.1/Vβ8.2 positive lymphocytes, overview (E), and detailed section (F).

References

1. Matsumoto, I., A. Staub, C. Benoist, and D. Mathis. 1999. Arthritis provoked by linked T and B cell recognition of a glycolytic enzyme. *Science*. 286:1732–1735.
2. Steinhoff, U., V. Brinkmann, U. Klemm, P. Aichele, P. Seiler, U. Brandt, P.W. Bland, I. Prinz, U. Zügel, and S.H.E. Kaufmann. 1999. Autoimmune intestinal pathology induced by hsp60-specific CD8 T cells. *Immunity*. 11:349–358.
3. Zügel, U., B. Schoel, S. Yamamoto, H. Hengel, B. Morein, and S.H. Kaufmann. 1995. Crossrecognition by CD8 T cell receptor alpha beta cytotoxic T lymphocytes of peptides in the self and the mycobacterial hsp60 which share intermediate sequence homology. *Eur. J. Immunol.* 25:451–458.
4. Grant, E.P., M.T. Michalek, A.L. Goldberg, and K.L. Rock. 1995. Rate of antigen degradation by the ubiquitin-proteasome pathway influences MHC class I presentation. *J. Immunol.* 155:3750–3758.
5. Cerundolo, V., A. Benham, V. Braud, S. Mukherjee, K. Gould, B. Macino, J. Neefjes, and A. Townsend. 1997. The proteasome-specific inhibitor lactacystin blocks presentation of cytotoxic T lymphocyte epitopes in human and murine cells. *Eur. J. Immunol.* 27:336–341.
6. Rock, K.L., C. Gramm, L. Rothstein, K. Clark, R. Stein, L. Dick, D. Hwang, and A.L. Goldberg. 1994. Inhibitors of the proteasome block the degradation of most cell proteins and the generation of peptides presented on MHC class I molecules. *Cell*. 78:761–771.
7. Schwarz, K., R. de Giuli, G. Schmidtke, S. Kostka, M. van den Broek, K.B. Kim, C.M. Crews, R. Kraft, and M. Groettrup. 2000. The selective proteasome inhibitors lactacystin and epoxomicin can be used to either up- or down-regulate antigen presentation at nontoxic doses. *J. Immunol.* 164:6147–6157.
8. Groll, M., L. Ditzel, J. Lowe, D. Stock, M. Bochtler, H.D. Bartunik, and R. Huber. 1997. Structure of 20S proteasome from yeast at 2.4 A resolution. *Nature*. 386:463–471.
9. Akiyama, K., S. Kagawa, T. Tamura, N. Shimbara, M. Takashina, P. Kristensen, K.B. Hendil, K. Tanaka, and A. Ichihara. 1994. Replacement of proteasome subunits X and Y by LMP7 and LMP2 induced by interferon-gamma for acquirement of the functional diversity responsible for antigen processing. *FEBS Lett*. 343:85–88.
10. Fruh, K., M. Gossen, K. Wang, H. Bujard, P.A. Peterson, and Y. Yang. 1994. Displacement of housekeeping proteasome subunits by MHC-encoded LMPs: a newly discovered mechanism for modulating the multicatalytic proteinase complex. *EMBO J.* 13:3236–3244.
11. Nandi, D., H. Jiang, and J.J. Monaco. 1996. Identification of MECL-1 (LMP-10) as the third IFN-gamma-inducible proteasome subunit. *J. Immunol.* 156:2361–2364.
12. Boes, B., H. Hengel, T. Ruppert, G. Multhaup, U.H. Koszinowski, and P.M. Kloetzel. 1994. Interferon gamma stimulation modulates the proteolytic activity and cleavage site preference of 20S mouse proteasomes. *J. Exp. Med*. 179:901–909.
13. Gaczynska, M., K.L. Rock, T. Spies, and A.L. Goldberg. 1994. Peptidase activities of proteasomes are differentially regulated by the major histocompatibility complex-encoded genes for LMP2 and LMP7. *Proc. Natl. Acad. Sci. USA*. 91: 9213–9217.
14. Klose, J., and U. Kobalz. 1995. Two-dimensional electrophoresis of proteins: an updated protocol and implications for a functional analysis of the genome. *Electrophoresis*. 16:1034–1059.
15. Lamer, S., and P.R. Jungblut. 2001. Matrix-assisted laser desorption-ionization mass spectrometry peptide mass fingerprinting for proteome analysis: identification efficiency after on-blot or in-gel digestion with and without desalting procedures. *J. Chromatogr.* 752:311–322.
16. Seelig, A., B. Boes, and P.M. Kloetzel. 1993. Characterization of mouse proteasome subunit MC3 and identification of proteasome subtypes with different cleavage characteristics. Proteasome subunits, proteasome subpopulations. *Enzyme Protein*. 47:330–342.
17. Arribas, J., P. Arizti, and J.G. Castano. 1994. Antibodies against the C2 COOH-terminal region discriminate the active and latent forms of the multicatalytic proteinase complex. *J. Biol. Chem*. 269:12858–12864.
18. Covi, J.A., J.M. Belote, and D.L. Mykles. 1999. Subunit compositions and catalytic properties of proteasomes from developmental temperature-sensitive mutants of *Drosophila melanogaster*. *Arch. Biochem. Biophys*. 368:85–97.
19. Kania, M.A., G.N. Demartino, W. Baumeister, and A.L. Goldberg. 1996. The proteasome subunit, C2, contains an important site for binding of the PA28 (11S) activator. *Eur. J. Biochem*. 236:510–516.
20. Zhang, Z., N. Torii, A. Furusaka, N. Malayaman, Z. Hu, and T.J. Liang. 2000. Structural and functional characterization of interaction between hepatitis B virus X protein and the proteasome complex. *J. Biol. Chem*. 275:15157–15165.
21. Groll, M., M. Bajorek, A. Kohler, L. Moroder, D.M. Rubin, R. Huber, M.H. Glickman, and D. Finley. 2000. A gated channel into the proteasome core particle. *Nat. Struct. Biol.* 7:1062–1067.
22. Kuckelkorn, U., S. Frentzel, R. Kraft, S. Kostka, M. Groettrup, and P.M. Kloetzel. 1995. Incorporation of major histocompatibility complex—encoded subunits LMP2 and LMP7 changes the quality of the 20S proteasome polypeptide processing products independent of interferon-gamma. *Eur. J. Immunol.* 25:2605–2611.
23. Kloetzel, P.M. 2001. Antigen processing by the proteasome. *Nat. Rev. Mol. Cell Biol*. 2:179–187.
24. Emmerich, N.P., A.K. Nussbaum, S. Stevanovic, M. Priemer, R.E. Toes, H.G. Rammensee, and H. Schild. 2000. The human 26 S and 20 S proteasomes generate overlapping but different sets of peptide fragments from a model protein substrate. *J. Biol. Chem*. 275:21140–21148.
25. Craiu, A., T. Akopian, A. Goldberg, and K.L. Rock. 1997. Two distinct proteolytic processes in the generation of a major histocompatibility complex class I-presented peptide. *Proc. Natl. Acad. Sci. USA*. 94:10850–10855.
26. Stoltze, L., M. Schirle, G. Schwarz, C. Schroter, M.W. Thompson, L.B. Hersh, H. Kalbacher, S. Stevanovic, H.G. Rammensee, and H. Schild. 2001. Two new proteases in the MHC class I processing pathway. *Nat. Immunol.* 1:413–418.
27. Lucchiari-Hartz, M., P.M. van Endert, G. Lauvau, R. Maier, A. Meyerhans, D. Mann, K. Eichmann, and G. Niedermann. 2000. Cytotoxic T lymphocyte epitopes of HIV-1 Nef: generation of multiple definitive major histocompatibility complex class I ligands by proteasomes. *J. Exp. Med*. 191:239–252.
28. Dahlmann, B., T. Ruppert, P.M. Kloetzel, and L. Kuehn. 2001. Subtypes of 20S proteasomes from skeletal muscle. *Biochimie*. 83:295–299.
29. Skoberne, M., R. Holtappels, H. Hof, and G. Geginat. 2001. Dynamic antigen presentation patterns of *Listeria monocytogenes*-derived CD8 T cell epitopes in vivo. *J. Immunol.* 167: 2209–2218.